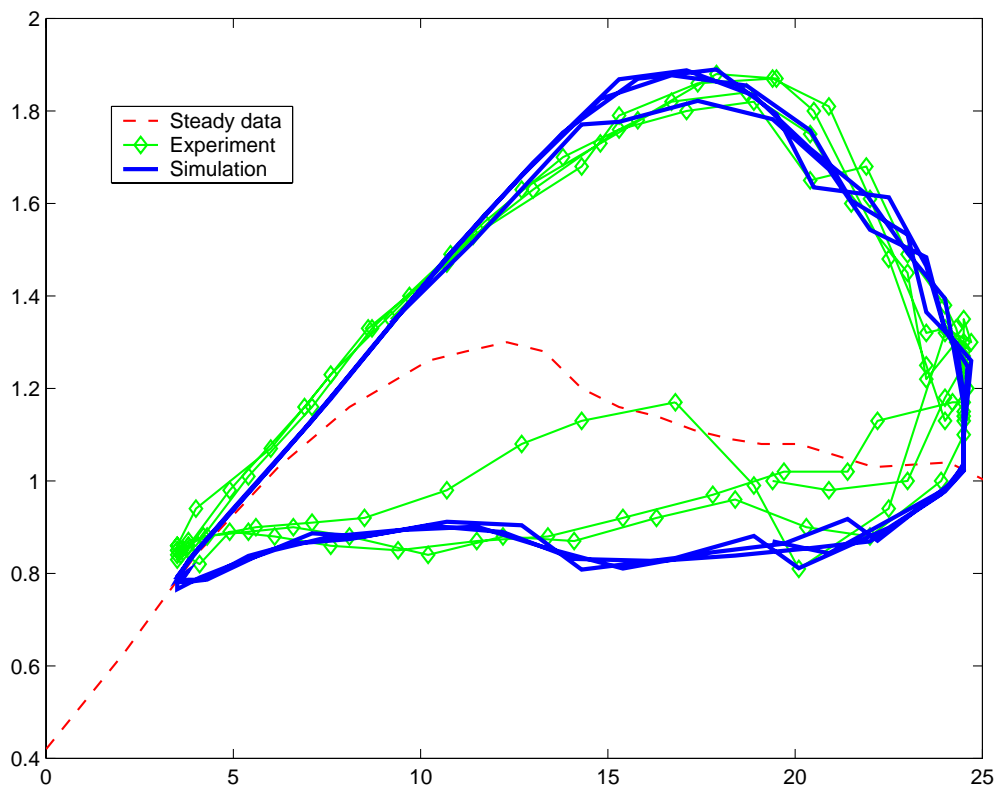


DYNSTALL: Subroutine Package with a Dynamic stall model

Anders Björck





THE AERONAUTICAL RESEARCH INSTITUTE OF SWEDEN
Box 11021, SE-161 11 Bromma, Sweden
Phone +46 8 634 10 00, Fax +46 8 25 34 81

Summary

A subroutine package, called DYNSTALL, for the calculation of 2D unsteady airfoil aerodynamics is described.

The subroutines are written in FORTRAN.

DYNSTALL is a basically an implementation of the Beddoes-Leishman dynamic stall model. This model is a semi-empirical model for dynamic stall. It includes, however, also models for attached flow unsteady aerodynamics. It is complete in the sense that it treats attached flow as well as separated flow. Semi-empirical means that the model relies on empirically determined constants. Semi because the constants are constants in equations with some physical interpretation. It requires the input of 2D airfoil aerodynamic data via tables as function of angle of attack.

The method is intended for use in an aeroelastic code with the aerodynamics solved by blade/element method.

DYNSTALL was written to work for any 2D angles of attack relative to the airfoil, e.g. flow from the rear of an airfoil.

Content

1	INTRODUCTION	9
2	THE BEDDOES-LEISHMAN MODEL.....	11
2.1	ATTACHED FLOW	12
2.2	SEPARATED FLOW.....	15
2.3	THE MODEL IN STEPS	17
2.4	SEMI-EMPIRICAL CONSTANTS.....	19
3	THE DYNSTALL UNSTEADY AIRFOIL AERODYNAMICS MODEL	21
3.1	A CHANGE TO WORK IN THE WIND REFERENCE SYSTEM	21
3.2	ATTACHED FLOW	22
3.2.1	<i>The angle of attack.....</i>	22
3.2.2	<i>Attached flow equations (LPOTMETH=3)</i>	24
3.2.3	<i>Shed wake effects with account for a varying lift curve slope (LPOTMETH=4).....</i>	26
3.3	SEPARATED FLOW.....	28
3.3.1	<i>A shift in the angle of attack.....</i>	28
3.3.2	<i>Lift as function of the separation point position.....</i>	30
3.3.2.1	<i>The Øye separation point model (lfmeth=2).....</i>	30
3.3.2.2	<i>A version of the Kirchoff flow (lfmeth=4).....</i>	32
3.3.3	<i>Vortex lift (lvormeth=2)</i>	34
3.3.4	<i>An alternative version of vortex lift (lvormeth=1).....</i>	34
3.4	UNSTEADY DRAG.....	35
3.5	UNSTEADY PITCHING MOMENT	37
3.6	WAYS TO MAKE THE MODEL WORK FOR ALL ANGLES OF ATTACK	37
3.7	ROBUSTNESS OF THE DYNSTALL-METHODS	38
3.7.1	<i>Methods that work for all angles of attack.....</i>	39
4	INPUT TO THE FORTRAN SUBROUTINE PACKAGE.....	41
4.1	SUBROUTINES	41
4.2	CONVENTIONS FOR VARIABLE NAMES.....	42
4.3	ABOUT HISTORY OF VARIABLE NAMES.....	42
4.4	COMMUNICATION WITH THE SUBROUTINES.....	42
4.5	COMMON AREAS IN DYNCL_C.INC	43
4.5.1	<i>Storage of static airfoil data.</i>	43
4.5.1.1	<i>Range of angle of attack in input airfoil tables.</i>	45
4.5.1.2	<i>Lift curve slope and zero lift angle of attack.....</i>	45
4.5.2	<i>Choices between submodels.....</i>	46
4.5.3	<i>Coefficients and time constants.....</i>	47
4.5.4	<i>Variables used for state variables and other variables needed for internal communication.....</i>	47

4.5.5	<i>Variables in common areas that must be set at each time step outside of the DYNSTALL-package</i>	48
4.6	GENERATION OF FNSTIN, CNINVIN AND CNSEPIN TABLES.....	48
5	SUB-METHODS AND VALUES FOR SEMI-EMPIRIC CONSTANTS	49
5.1	AN OPTIMIZATION STUDY TO FIND OPTIMUM VALUES	49
5.2	LCDDYN.....	50
5.3	EFFECTS OF VARYING VELOCITY ON THE SEPARATION POINT	50
5.4	RECOMMENDED VALUES OF SUB-MODELS AND SEMI-EMPIRICAL PARAMETERS	50
5.4.1	<i>Effect on aerodynamic damping, fatigue and extreme loads</i>	51
5.4.1.1	Damping of flap-wise vibrations in stall.....	51
5.4.1.2	Damping of edge-wise vibrations in stall	51
5.4.1.3	Extreme loads	52

Symbols and notations

c	Chord
c_v	Vortex feed (equation (2.2.3) and (3.3.3.1))
$C_{N\alpha}$	Lift curve slope.[1/rad] Same as $C_{L\alpha}$
$C_{L\alpha}$	Lift curve slope.[1/rad] Same as $C_{N\alpha}$
C_L	Lift coefficient
C_D	Drag coefficient
C_M	Moment coefficient
C_T	Tangential force coefficient.
C_N	Normal force coefficient.

Note that capital subscripts for lift, drag , pitching moment , tangential and normal force coefficients are used even though it refers to two-dimensional quantities. Capital letters for the subscripts is not to mix with other indices, e.g. n for time step number

f, f'	separation point location
IB	Index for blade number IB
IR	Index for radial element IR
q	Pitch rate [rad/s]
u_p	Plunge velocity (equation 3.2.2.7))
V_{rel}	Velocity relative to two-dimensional airfoil element.
w	Normal component of velocity relative to the airfoil (equation (3.2.2.2))
s	Dimensionless time, Dimensionless with half-chord and V_{rel}
t	Time
α	Angle of attack
α_E	Effective angle of attack (equation (2.1.6) and equation (3.2.2.5))
α_i	Shed wake induced angle of attack (equation (2.1.5))

α_g	Geometric angle of attack (equation (3.2.1.1))
α_{75}	$\frac{3}{4}$ chord angle of attack (equation (3.2.1.2))
Γ	Circulation [m^2 / s]
T_p	Time constant for leading edge pressure lag (equation (2.3.1))
T_f	Time constant for separation point position lag (equation (2.2.2))
T_v	Time constant for vortex lift decay (equation (2.2.4))
2D	Two-dimensional
3D	Three- dimensional

Subscripts

qs	“quasi steady” values
n	time step n
∞	Free stream conditions or conditions at infinity
I	Impulsive loads
c	Circulatory loads
pot	Potential loads (sum of impulsive and circulatory loads)
v	Vortex part of lift, drag et.c.
f	Related to separation point location
$stat$	Static (or quasi-static) conditions
dyn	Unsteady conditions

1 Introduction

This report describes the unsteady profile aerodynamics model used in the blade element/momentum (BEM) code AERFORCE [1].

Unsteady aerodynamics is of great importance for wind turbines. Both for flow in the attached flow angle of attack region and for flow in the separated flow region.

Most attention is often given to the unsteady separated flow affects, commonly named “dynamic stall”. The stalling behavior of an airfoil will be quite different from its steady stalling behavior if the angle attack is changed fast enough. The maximum lift coefficient can e.g. significantly exceed its static value. For wind turbines, dynamic stall also largely affects the aerodynamic damping in stall. Generally the damping would be largely under-predicted if steady stall data were used in aeroelastic calculations. Also, for yawed turbines, dynamic stalling plays a great role with increased $C_{L,max}$ and different phase of the aerodynamic forces as a function of rotor azimuth angle relative to using steady data. Many papers and reports have been written dealing with dynamic stall for wind turbines. A recent paper is [2] in which further references can found. Dynamic stall has also been subject of two EC research projects [3] and [4].

Unsteady aerodynamics is, however, also important for attached flow. Unsteady aerodynamics effects are important e.g. for stability calculations at turbine over-speeding, for blade-tower interactions and for fast pitching action.

The model in the DYNSTALL-package is an implementation of the Beddoes-Leishman dynamic stall model described in e.g. [5], [6] and [7]. This model is a 2D semi-empirical model for dynamic stall. It includes, however, also models for attached flow unsteady aerodynamics. It is thus complete in the sense that it treats attached flow as well as separated flow

1.1 Structure of the report

The Beddoes-Leishman model in its original version is presented in chapter 2. Changes to this model that are introduced in the FFA DYNSTALL version are described in chapter 3.

In chapter 4 details in the Fortran implementation are given.

Finally some recommendations on the use are given in chapter 5.

2 The Beddoes-Leishman model

The Beddoes-Leishman model is a semi-empirical model. Semi-empirical means that the model relies on empirically determined constants. Semi because the constants are constants in equations with some physical interpretation.

The model is based on tables of steady aerodynamic data ($C_L(\alpha)$, $C_D(\alpha)$ and $C_M(\alpha)$).

The unsteady behavior is described by different processes as e.g. the shed wake effect on the inflow and a dynamic delay in the separation process. The different dynamic processes are modeled as differential equations that need user-set values for constants to get best agreement with experiments or theoretical models.

The Beddoes-Leishman model can be described as an indicial response model for attached flow extended with models for separated flow effects and vortex lift. The forces are computed as normal force, tangential force and pitching moment. Indicial response means that the model works with a series of small disturbances.

The attached flow part reproduces the linear theory of [9] for force response for a pitching airfoil, a plunging airfoil and the wind gust case. See e.g. [8], section 2.6 for a general description of the attached flow solution.

The unsteady 2D airfoil aerodynamic response scales with time made dimensionless with speed relative to the airfoil and the chord of the airfoil. The time in the equations¹ is therefore replaced with dimensionless time:

¹ One exception is the “impulsive loads” which scale with the chord and the speed of sound

$$s = \frac{V_{rel} \cdot t}{c/2} \quad (2.1)$$

The model uses steady $C_L(\alpha)$ and $C_D(\alpha)$ data as input for a specific airfoil for which the dynamic forces are to be calculated. In the Beddoes-Leishman model, the forces in the body fixed system, C_N and C_T , are used, where:

$$C_N = C_L \cos(\alpha) + C_D \sin(\alpha) \quad (2.2)$$

$$C_T = C_D \cos(\alpha) - C_L \sin(\alpha) \quad (2.3)$$

The Beddoes-Leishman model also treats the unsteady effects on the pitching moment. Dynamic stall has a dramatic effect on the pitching moment and on the damping for pitch-oscillations. This is very important for helicopter rotors but is less important for wind turbine blades. The treatment of the pitching moment is therefore left out in the description below.

The description below of the Beddoes-Leishman model follows as far as how to solve equations, the methods described in [5]. Alternative solutions using a state-space model are described in [7].

2.1 Attached flow

For attached flow, two different aspects are modeled. When the bound vorticity of the airfoil is time varying, vorticity is shed in the wake. This shed vorticity induces a flow over the airfoil, so that the airflow sensed by the airfoil is not the free stream velocity. If for example the lift (and the bound circulation of the airfoil) has been increasing for some time, then the shed wake will cause a down-wash over the airfoil, resulting in less lift than would be anticipated in steady flow.

The other effect is the “impulsive load” effect. This effect is also called the apparent mass effect. This effect causes a lift force for a fast pitch or fast downward plunge motion.

The shed wake effects influences the “circulatory lift”. The “impulsive loads” are added to get the total attached flow lift (lift is here the same as normal force since the angle of attack is assumed small for the attached flow part)

The flow conditions are simulated by the superposition of indicial responses.

Circulatory part

For the “circulatory” part this is written as:

$$\Delta C_{N,c} = [C_{N\alpha}(M) \cdot \phi_c(s, M)] \Delta \alpha \quad (2.1.1)$$

The indicial response for the shed wake effects is approximated by

$$\phi_c = 1 - A_1 \exp(-b_1 \beta s) - A_2 \exp(-b_2 \beta s) \quad (2.1.2)$$

where

$$\beta = \sqrt{1 - M^2}$$

Suggestions for constants A_1 , A_2 , b_1 and b_2 are given in [5] as

$$A_1=0.3 \quad A_2=0.7 \quad b_1=0.14 \quad \text{and} \quad b_2=0.53$$

The shed wake effect is computed by using a lagged “effective” angle of attack: $\alpha_E = \alpha - \alpha_i$ where α_i can be seen as the shed wake induced angle of attack.

The numerical method to compute α_i given in [5] is for the n :th time step:

$$X_n = X_{n-1} \exp(-b_1 \beta \Delta s) + A_1 \Delta \alpha_n \exp(-b_1 \beta \Delta s / 2) \quad (2.1.3)$$

$$Y_n = Y_{n-1} \exp(-b_2 \beta \Delta s) + A_2 \Delta \alpha_n \exp(-b_2 \beta \Delta s / 2) \quad (2.1.4)$$

$$\alpha_{i,n} = X_n + Y_n \quad (2.1.5)$$

The circulatory lift (or really the normal force) is taken as

$$C_{N,c,n} = C_{N\alpha} (\alpha_{E_n} - \alpha_0) \quad (2.1.6)$$

where $\alpha_{E_n} = \alpha_n - \alpha_{i_n}$

Impulsive load

The impulsive lift is calculated from piston theory:

$$\Delta C_{N,I} = \left[\frac{4}{M} \phi_I(s, M) \right] \Delta \alpha \quad (2.1.7)$$

The transfer function is approximated by

$$\phi_I(t) = e^{\frac{-t}{K_\alpha \cdot T_I}} \quad (2.1.8)$$

where

$T_I = \frac{c}{a}$ where c is the chord and a is the speed of sound.

K_α is a function of the mach number as given in [5].

Equation (2.1.7) and (2.1.8) are solved to give the impulsive lift at time step n as

$$C_{N,I,n} = \frac{4 \cdot K_\alpha \cdot c}{V_{rel}} \left(\frac{\Delta \alpha_n}{\Delta t} - D_n \right) \quad (2.1.9)$$

where the deficiency function is given by

$$D_n = D_{n-1} \cdot e^{\frac{-\Delta t}{K_\alpha T_l}} + \left(\frac{\Delta \alpha_n - \Delta \alpha_{n-1}}{\Delta t} \right) \cdot e^{\frac{-\Delta t}{2K_\alpha T_l}} \quad (2.1.10)$$

Total attached flow lift

The total attached flow lift (potential flow lift) is then obtained by adding the circulatory and impulsive lift.

$$C_{N,pot} = C_{N,c} + C_{N,I} \quad (2.1.11)$$

2.2 Separated flow

The simulated separated flow effects are: 1) a dynamic delay in the movement of the boundary layer separation position and 2) the dynamic leading edge stall with a vortex travelling downstream along the chord.

The first part is based on the physical concept that C_N is a function of the separation point position and that the movement of the separation point has a dynamic delay.

The second part results in “vortex lift” that is added to the normal force. The “vortex lift” has a dramatic effect on the pitching moment. Much attention has therefore been given to estimate the conditions at which the vortex lift is shed over the airfoil and the speed at which it travels. The condition at which the dynamic stall vortex is shed, is in the model controlled by the condition that the normal force coefficient exceeds a certain value. The condition at when leading edge stall occurs, is really controlled by a critical leading edge pressure coefficient. To link this critical leading edge pressure coefficient to C_N , the model works with a lagged C_N . (See e.g. [5] for details and [10] for comments on the difference between plunge and pitching motion).

Delay in the movement of the separation point.

To model the effect of the delay in the movement of the separation point position requires a $C_N(f)$ relationship. One such relationship is the Kirchhoff flow model as described in [5].

The relationship between f and C_N in the Kirchhoff flow model is:

$$C_N(\alpha) = C_{N\alpha} \cdot 0.25 \cdot \left(1 + \sqrt{f(\alpha)}\right)^2 (\alpha - \alpha_0) \quad (2.2.1)$$

Where α_0 is the angle of attack for zero lift and $C_{N\alpha}$ is the attached flow lift curve slope. f is the chord-wise position of separation. f is made dimensionless with the chord length and $f = 1$ represents fully attached flow and $f = 0$ represents fully separated flow.

The static $f(\alpha)$ can in principle be obtained as a table by solving equation (2.2.1) with the steady $C_N(\alpha)$ curve. However, in the Beddoes-Leishman model as described in [5], a parametric $f(\alpha)$ -curve that is a best fit to the steady $C_N(\alpha)$ curve is suggested.

In order to obtain the dynamic value of the position of separation point, the model is that the dynamic f lags behind its steady value according to a first order lag equation:

$$\frac{df}{ds} = \frac{f_{stat} - f}{T_f} \quad (2.2.2)$$

s is here the dimensionless time from equation (2.1). T_f is a semi-empirical time constant (time constant in the s -space).

By using the dimensionless time, s , the model for the lag in the separation point works for any frequency of oscillation or any time history with T_f as a constant.

The dynamic lift, $C_{N,f}$, is obtained from the Kirchhoff flow equation with the dynamic value of the separation point position.

Vortex lift

The model further includes a model for vortex lift, with the amount of vortex lift determined by a time-lag function with a time constant, T_v . It is assumed that the vortex lift contribution can be viewed as an excess circulation, which is not shed into the wake until some critical condition is reached. The vortex lift, $C_{N,v}$ is determined by the following equations:

The “feed” of vortex lift is proportional to the difference in unsteady circulatory lift and the non-linear lift given from the Kirchoff flow equation with the dynamic value of the separation point position.

$$c_v = C_{N,c} - C_{N,f} \quad (2.2.3)$$

At the same time, the total accumulated vortex lift is allowed to decay exponentially with time, but may also be updated with new vortex lift feed.

$$\frac{dC_{N,v}}{ds} = \frac{\frac{dc_v}{ds} - C_{N,v}}{T_v} \quad (2.2.4)$$

The last equation is solved at the n :th time step as:

$$C_{N,v,n} = C_{N,v,n-1} e^{\frac{-\Delta s}{T_v}} + (c_{v,n} - c_{v,n-1}) e^{\frac{-\Delta s}{2T_v}} \quad (2.2.5)$$

Conditions for when the addition of new vortex lift feed should stop and conditions for how T_v should vary with f and the position of the travelling vortex, are given in [5].

2.3 The model in steps

The model works as an open loop model so that the whole model is programmed in steps in which the output from earlier sub-models are input to the next sub-model.

Step 1

Calculate attached flow effects (impulsive loads and shed wake effects) => effective angle of attack, α_E and impulsive force $C_{N,imp}$

Step 2

Compute a shift in angle of attack due to the lag in leading edge pressure response.

$$\frac{dC'_{N,pot}}{ds} = \frac{C_{N,pot} - C'_{N,pot}}{T_p} \quad (2.3.1)$$

Where T_p is an empirical time constant.

$C'_{N,pot}$ is then used to get substitute value of the effective angle of attack:

$$\alpha_f = \frac{C'_{N,pot}}{C_{N\alpha}} - \alpha_0 \quad (2.3.2)$$

Step 3

Use $f_{stat} = f_{stat}(\alpha_f)$ and compute the unsteady separation point position, f_{dyn} , from the lag equation for the separation point. Use f_{dyn} in the Kirchoff $C_n(f)$ relationship to obtain a dynamic value of the normal force coefficient, $C_{N,f}$.

Step 4

Compute vortex lift from equations (2.2.3) and (2.2.4)

Step 5

Add components to get total normal force:

$$C_N = C_{N,I} + C_{N,f} + C_{N,v}$$

2.4 Semi-empirical constants

The main semi-empirical constants are the three time constants for the leading edge pressure lag, T_p , the lag in separation point movement, T_f , and for the vortex lift decay, T_v .

Values for these constants are suggested in [5].

In the Beddoes-Leishman model, semi-empirical constants are also needed to control the conditions for the dynamic stall vortex shedding and to control its travel speed. For an explanation of these constants, $C_{N,l}$ and T_{vl} , see [5].

In [5], several conditions are also suggested for which some of the time constants should be halved or doubled depending on e.g. the value of the separation point position, f or the position of the traveling vortex.

3 The DYNSTALL unsteady airfoil aerodynamics model

The model in the DYNSTALL-package is an implementation of the Beddoes-Leishman model, but with a few changes made relative to the description above and as given in [5], [6] and [7].

The changes to the model are made to make it more robust for use in wind turbine aeroelastic simulations with turbulent wind. The model now works for angles of attack in the whole range $[-180^\circ, 180^\circ]$. Some changes were also introduced during the “Stallvib” project [3] where the unsteady aerodynamics for lead-lag blade oscillations were studied.

In the following text, when there is mention of the current version of DYNSTALL it is referred to the subroutines in the files:

dyncl_c.f, v_esti_c.f and vo_sub_c.f

3.1 A change to work in the wind reference system

The Beddoes-Leishman model as described in [5] works in the body fixed frame. Forces are described in the direction normal to the airfoil, C_N , and in the chord-wise direction, C_T . The attached flow part originates from linearised theory at small angles of attack where $\alpha \approx \sin(\alpha) \approx \tan(\alpha)$, so that no distinction can really be made between C_N and C_L in that theory. For the non-linear part (separated flow) the Beddoes-Leishman model also works with C_N and C_T . There might be advantages by setting up the separated flow equations in the body fixed system but difficulties arise when the dynamic behavior of C_T at high angles of attack should be modeled with the model from [5].

The current version of DYNSTALL therefore uses the wind reference system. Most equations in C_N in the Beddoes-Leishman

model are treated as being equations in C_L . One exception is that the vortex lift still is treated as being normal to the airfoil chord.

One advantage of working in the wind reference system is that the delay in the separation point position automatically affects the tangential force. This happens since C_T has a rather large component of C_L at stall angles of attack. Most of the effect of the dynamic delay of the separation point on C_T is therefore automatically a result of the delay in the lift. The effect of the dynamic delay of the separation point on C_D is also modeled in DYNSTALL. Still the main effect on C_T comes from the lift part at stall angles of attack.

The vortex lift is, however, assumed to act only in the normal force direction. An increase of T_f will increase the dynamic stall loop width of the $C_N(\alpha)$ -curve as well as the $C_T(\alpha)$ -curve, whereas an increase of T_v will increase only the width of the $C_N(\alpha)$ -curve and leave the $C_T(\alpha)$ -curve unaffected. The fact that T_v only affects C_N makes it possible to tune the time constants, T_f and T_v , to obtain a good fit to both the $C_T(\alpha)$ as well as the $C_N(\alpha)$ -curve.

3.2 Attached flow

The attached flow equations are basically the same as in [5] and given in chapter 2 above.

In DYNSTALL, two methods are however available for how to calculate the shed wake effect. In the alternative method explained in section 3.2.2 the shed wake effect is made a function of the actual circulation history and not the circulation history that would occur for attached flow as in the original model.

3.2.1 The angle of attack

The angle of attack that is input to the equations includes the pitch rate effects.

A geometrical angle of attack, α_g , is defined as the angle between the chord-line and the relative velocity to the airfoil. The relative velocity to the airfoil includes here the translation motion of the airfoil. No difference is hence made between the airfoil moving in still air or the airfoil being at a stand-still at an incidence in an airflow.

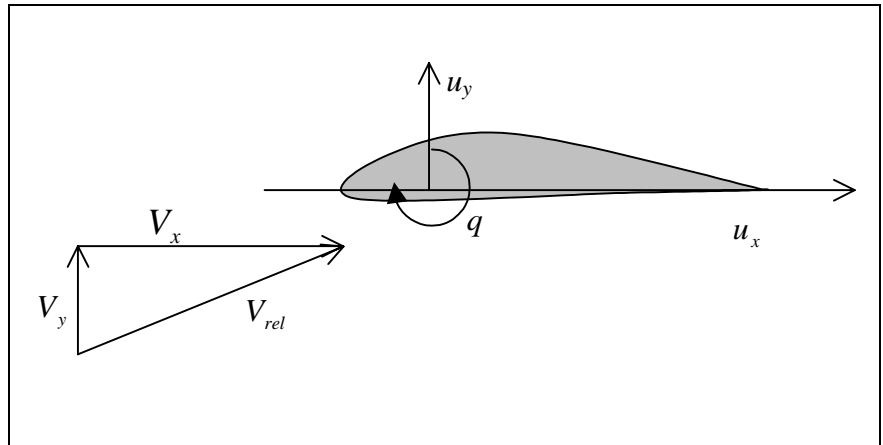


Figure 1

In the picture above, the airfoil is at a geometrical incidence and also has a heaving velocity, u_y , and a lead/lag velocity, u_x . α_g is then calculated from the angle of the relative velocity to the chord line as:

$$\tan(\alpha_g) = \frac{V_y - u_y}{V_x - u_x} \quad (3.2.1.1)$$

In order to automatically include the pitch rate effect in the lift, the angle of attack at the $\frac{3}{4}$ chord position can be used. The DYNSTALL package therefore also works with the angle of attack at the $\frac{3}{4}$ chord position. This angle of attack is called α_{75} .

With the velocity relative to the airfoil, V_{rel} , and the pitch rate q , then

$$\alpha_{75} = \alpha_g + \frac{c \cdot q}{2 \cdot V_{rel}} \quad (3.2.1.2)$$

α_{75} is then used for α in equations for the circulatory lift in section 2.1.

3.2.2 Attached flow equations (LPOTMETH=3)

The attached flow equations are available in two versions. The choice of version is controlled by an input parameter LPOTMETH. (LPOTMETH=1 used to be the attached flow equations in section 2.1. but is no longer implemented since it is equivalent to LPOTMETH=3 for constant V_{rel})

Circulatory part

The equations are reformulated to work with the normal velocity at the $\frac{3}{4}$ point chord position. This is the same as reformulating the equations in circulation rather than in lift coefficient. With this formulation, the circulatory effect will be correct for lead-lag motions and for a varying wind speed.

Equation (2.1.1) then becomes

$$\Delta\Gamma = \left[\frac{c}{2} \cdot C_{L\alpha} \cdot \phi_c \right] \Delta w \quad (3.2.2.1)$$

w is the normal component of the relative velocity to the airfoil at the $\frac{3}{4}$ point chord position. In this case the normal direction is taken as normal to the zero-lift line and the small angle approximation is used.

$$w = \frac{(\alpha_{75} - \alpha_0)}{V_{rel}} \quad (3.2.2.2)$$

The equations to solve for the effective angle of attack are then at the n :th time step

$$X_n = X_{n-1} \exp(-b_1 \beta \Delta s) + A_1 \Delta w_n \exp(-b_1 \beta \Delta s / 2) \quad (3.2.2.3)$$

$$Y_n = Y_{n-1} \exp(-b_2 \beta \Delta s) + A_2 \Delta w_n \exp(-b_2 \beta \Delta s / 2) \quad (3.2.2.4)$$

$$\alpha_E = (\alpha_{75} - X_n - Y_n) / V_{rel} + \alpha_0 \quad (3.2.2.5)$$

This method is obtained by choosing LPOTMETH=3.

$\beta = \sqrt{1 - M^2}$ is in the current version set to unity since Mach number effects for wind turbines for the shed wake effect are assumed small.

In order to avoid queer results when the linearised theory is used at high angles of attack, Δw in equations (3.2.2.3) and (3.2.2.4) are factored with a factor *fade*. Where

$$fade = \cos^2(\alpha_{75}) \quad (3.2.2.6)$$

Impulsive load

The impulsive load should be calculated from the airfoil “plunge” velocity at the $\frac{3}{4}$ point chord position. This plunge velocity could come from airfoil plunging but could also be due to a pitch rate induced velocity at the $\frac{3}{4}$ point chord position.

With, u_p as the velocity of the $\frac{3}{4}$ point chord position directed in the negative y-direction, the equations for impulsive loads at the n :th time step are written:

$$C_{L,I,n} = \frac{4 \cdot K_\alpha \cdot c}{V_{rel,n} \cdot U_{mean}} \left(\frac{\Delta u_{p,n}}{\Delta t} - D_n \right) \quad (3.2.2.7)$$

with the deficiency function given by

$$D_n = D_{n-1} \cdot e^{\frac{-\Delta t}{K_\alpha T_I}} + \left(\frac{\Delta u_{p,n} - \Delta u_{p,n-1}}{\Delta t} \right) \cdot e^{\frac{-\Delta t}{2K_\alpha T_I}} \quad (3.2.2.8)$$

and U_{mean} is the mean of V_{rel} during the current and the previous time step.

K_α is in the current version of DYNSTALL set to 0.846 which is the value taken from [5] for $M=0.15$)

In the current version the impulsive normal force from equation (3.2.2.7) is taken as the impulsive lift force even though this is strictly correct only for $\alpha = 0$. In order to avoid queer results when the linearised theory is used at high angles of attack, Δu_p in equations (3.2.2.7) and (3.2.2.8) are factored with the factor *fade* from equation (3.2.2.6).

Pitching moment

The attached flow effects on the pitching moment are included by adding the impulsive load component to the pitching moment

$$C_{M,I} = \frac{C_{L,I}}{4} \quad (3.2.2.9)$$

3.2.3 Shed wake effects with account for a varying lift curve slope (LPOTMETH=4)

The above equations (used with LPOTMETH=3) are valid for attached flow. The shed wake effect is then calculated as if the flow were attached with a lift curve slope $C_{L\alpha}$, which is the lift curve slope around the zero lift angle of attack.

At angles of attack where the airflow starts to separate, the steady lift curve slope is no longer the same as for attached angles of attack. The lift may even decrease for an increase in angle of attack above stall.

It is then questionable if the shed wake effect (circulatory lift) could be calculated with a constant $C_{L\alpha}$.

One way to overcome this would be to calculate the shed wake effects from the circulation history (or lift history for constant V_{rel}) instead.

One problem is, however, that the lift is not known until the dynamic effects on the separation point positions is determined. This is solved by first calculating an estimate of $C_{L,f}$. This estimate, $C_{L,f,est}$, is calculated as in step 2 and 3 of the Beddoes-Leishman model but as explained in the sections on separated flow below.

The shed wake effect is then made a function of the difference in $C_{L,f,est}$ instead of the difference in α_{75} :

$$\Delta C_{L,f,est,n} = C_{L,f,est,n} - C_{L,f,est,n-1} \quad (3.2.3.1)$$

Further, $C_{L,f,est}$ must be based on the angle of attack without the shed wake effects if the model should give correct results for attached flow with the equations corresponding to (3.2.2.3)-(3.2.2.5). α_E is therefore set to α_{75} when the estimate of the dynamic lift, $C_{L,f,est}$, is calculated.

The method used to account for the fact that a reduced lift curve slope due to separated flow give reduced shed wake effects is: exchange $\Delta\alpha$ in equations (2.1.1)-(2.1.4) with $\Delta C_{L,f,est}/C_{L\alpha}$.

To, at the same time account for a varying circulation due to a varying velocity, Δw is used instead of $\Delta\alpha$ with w as in equation (3.2.1.2)

Δw to be put in equations (3.2.1.3)-(3.2.2.5) is then calculated, by differentiation, as

$$\Delta w = \frac{C_{L,f,est,mean}}{C_{L\alpha}} \cdot \Delta V_{rel} + \frac{\Delta C_{L,f,est}}{C_{L\alpha}} \cdot U_{mean} \quad (3.2.3.2)$$

with $C_{L,f,est,mean}$ being the mean of $C_{L,f,est}$ at the current and the previous time step.

As for LPOTMETH=3 Δw is multiplied with the factor *fade* from equation (3.2.2.6)

The so calculated effective angle of attack will be exactly the same as calculated with LPOTMETH=3 if the flow is attached. Attached flow means here that $f=1$ and $C_{L,f}(\alpha_E) = C_{L,stat}(\alpha_E)$.

For separated flow it will approximately account for the fact that the shed wake history is a function of the lift history rather than of the angle of attack history. The lift that is used to estimate the change on lift excludes the vortex lift since the vortex lift is considered not to affect the shed wake history.

The extra computing for LPOTMETH=4 relative to LPOTMETH=3, is that step 2 and 3 has to be run an extra time every time step to obtain $C_{L,f,est}$.

3.3 Separated flow

3.3.1 A shift in the angle of attack

The separation point position is statically a function of the angle of attack. What really influences the separation position is the pressure gradients in the boundary layer. To use the shifted angle of attack, α_f , as calculated from equation (2.3.2) is a way to account for the unsteady pressure gradient.

In DYNSTALL, the shift in the angle of attack to compensate for the lag in the leading edge pressure is used just as in the original model.

What is new to the FFA version, is to account for changes in the unsteady pressure gradient due to a varying free stream velocity. This was introduced during the STALLVIB project where lead-lag airfoil oscillations were studied [3], [11].

By studying the unsteady Bernoulli equation it can be seen that the pressure gradient along the airfoil will be different if the relative velocity is constant, increasing or decreasing (see [3] or [11]). If V_{rel}

is increasing, then the “effective” unsteady pressure gradient is found to be more favorable which in principle should result in less separation.

The question is how this effect on the pressure gradient and the corresponding effect on the separation point should be incorporated in the dynamic stall model. One way to do this is to see the resulting pressure gradients as gradients occurring at a different angle of attack. (A lower angle of attack for an accelerating free stream.) The point of separation, f , could then be determined using a corrected angle of attack as step 2b in the dynamic stall model. The assumption is that, at some angle of attack, $\alpha = \alpha + \Delta\alpha$, the pressure gradient for the case with varying V_{rel} , is similar to the pressure gradient at an angle of attack α , for the case with constant V_{rel} .

The equations to derive an estimate of the shift are given in [11] and [3]. The result is that the shift should be proportional to the dimensionless velocity change rate

$$\gamma = \frac{c}{2 \cdot V_{rel}^2} \cdot \frac{\partial V_{rel}}{\partial t} \quad (3.3.1.1)$$

The amount of shift is further controlled by an empirical parameter, f_u .

An estimate of $f_u = 0.5$ is given in [11].

Step 2, as in the description of the Beddoes-Leishman model in section 2.3, is in the FFA model:

Equation (2.3.1) is solved at the n :th time step as

$$dp_n = dp_{n-1} \cdot e^{\frac{-\Delta s}{T_p}} + (C_{N,pot,n} - C_{N,pot,n-1}) \cdot e^{\frac{-\Delta s}{2 \cdot T_p}} \quad (3.3.1.2)$$

and

$$C'_{N,pot,n} = C_{N,pot,n} - fade \cdot dp_n \quad (3.3.1.3)$$

The factor *fade* from equation (3.2.2.6) is included since the concept anyway breaks down at high angles of attack.

The shifted angle of attack α_f is taken from equation (2.3.2)

In the FFA-model the angle of attack is also shifted due to a varying velocity. α_f is therefore taken as

$$\alpha_f = \frac{C'_{N,pot}}{C_{N\alpha}} - \alpha_0 - \gamma \cdot f_u \quad (3.3.1.4)$$

3.3.2 Lift as function of the separation point position

The steady $C_l(\alpha)$ curve is in the dynamic stall model exchanged with a static $f(\alpha)$ relationship as explained in section 2.2.

The dynamic value (unsteady value) of the lift coefficient is then obtained by putting in a dynamic value of f in the $f(\alpha)$ relationship.

Two different types of $f(\alpha)$ can be used in DYNSTALL.

The choice between models is controlled by a variable `lfmeth`.

One model is the relationship introduced by Øye [12]. The other is a version of the Kirchhoff flow model.

In either case, the dynamic value of f is calculated by solving equation (2.2.2)

3.3.2.1 The Øye separation point model (lfmeth=2)

The formula linking C_L , f and α originating from Øye is used.

$$C_L = f \cdot C_{L,inv} + (1 - f) \cdot C_{L,sep} \quad (3.3.2.1.1)$$

This relationship requires steady curves of $C_{L,inv}(\alpha)$ and $C_{L,sep}(\alpha)$ in order to obtain either a steady $C_{L,stat}(\alpha)$ curve from a steady $f(\alpha)$ or a dynamic C_L from a dynamic f .

Equation (3.3.2.1.1) can be used to find a static $f(\alpha)$ relationship.

$$f_{stat}(\alpha) = \frac{C_{L,stat}(\alpha) - C_{L,sep}(\alpha)}{C_{L,inv}(\alpha) - C_{L,sep}(\alpha)} \quad (3.3.2.1.2)$$

$C_{L,inv}(\alpha)$, $C_{L,sep}(\alpha)$ and $f_{stat}(\alpha)$ are input to the program as tabulated values as function of α .

f should perhaps not be seen strictly as the separation point position, but rather as an interpolation factor between $C_{L,inv}(\alpha)$ and $C_{L,sep}(\alpha)$.

$C_{L,inv}$ could be taken as $C_{L\alpha}(\alpha - \alpha_0)$ and $C_{L,sep}$ as the curve for fully separated flow. The choice for the latter curve is more arbitrary. Øye [12] suggests a curve a curve starting with a slope of half value of the unseparated curve and gradually fitting to the steady $C_L(\alpha)$ curve at approximately 30° angle of attack.

To solve the differential equation (2.2.2), a value of f' is obtained from the $f_{stat}(\alpha)$ table with the angle of attack α_f as input.

(2.2.2) is then solved at the n :th time step as

$$df_n = df_{n-1} \cdot e^{\frac{-\Delta s}{T_f}} + (f'_n - f'_{n-1}) \cdot e^{\frac{-\Delta s}{2T_f}} \quad (3.3.2.1.3)$$

$$f_{dyn,n} = f'_n - df_n \quad (3.3.2.1.4)$$

$C_{L,f}$ is obtained from equation (3.3.2.1.1) as

$$C_{L,f}(\alpha_g) = f_{dyn} \cdot C_{L,inv}(\alpha_E) + (1 - f_{dyn}) \cdot C_{L,sep}(\alpha_E) \quad (3.3.2.1.5)$$

3.3.2.2 A version of the Kirchoff flow (lfmeth=4)

The Kirchoff flow equation written in equation (2.2.1) is used, but with some modifications.

First, C_L is used rather than C_N .

With $f=1$ the unmodified Kirchoff flow equation with C_L will give rather high values of C_L at large angles of attack. The DYNSTALL model should work over the whole range of angles of attack, and modifications are introduced to limit queer results at high angles of attack. The Kirchoff flow equation is therefore modified to limit C_L for $f=1$. Another fix is introduced to overcome the fact that if equation (2.2.1) (with C_N replaced by $C_{L,stat}$) is used to solve for the static $f_{stat}(\alpha)$, then this will only work as long as $C_{L,stat} < \frac{1}{4} \cdot C_{L\alpha}(\alpha - \alpha_0)$.

With $C_{L,inv} = C_{L\alpha} \cdot (\alpha - \alpha_0)$ and $C_{L,sep} = C_{L,inv} / 4$, the Kirchoff equation can be written to use the expressions $C_{L,inv}(\alpha)$ and $C_{L,sep}(\alpha)$ as in the Øye model.

$$C_L = C_{L,sep} + C_{L,inv} \cdot \frac{1}{4} \cdot (f + 2\sqrt{f}) \quad (3.3.2.2.1)$$

To limit C_L for $f=1$, equation (3.3.2.2.1) is modified for $\alpha > \alpha_c$.

If $\alpha > \alpha_c$, then the linear $C_{L,inv} = C_{L\alpha} \cdot (\alpha - \alpha_0)$ is exchanged for a sine curve that bends down almost to zero at 90° :

$$C_{L,inv} = \frac{1}{d_1} \cdot \sin(d_1 \cdot (\alpha - \alpha_0)) + d_2 \quad (3.3.2.2.2)$$

d_1 is a constant, somewhat arbitrarily, chosen to be 1.8. The constant d_2 assures continuity of the two $C_{L,inv}$ expressions at $\alpha = \alpha_c$ with

$$d_2 = C_{La} \left((\alpha_c - \alpha_0) - \frac{1}{d_1} \cdot \sin(\alpha_c - \alpha_0) \right) \quad (3.3.2.2.3)$$

The original Kirchoff curve is thus retained unchanged for $\alpha < \alpha_c$. $\alpha_c = 30^\circ$ is used in the AERFORCE package [1].

In order to get the equation to work for angles of attack where $\frac{1}{4} \cdot C_{L\alpha}(\alpha - \alpha_0) > C_{L,stat}$, $C_{L,sep}$ is then set to $C_{L,stat}$ and f_{stat} is then set to zero.

To construct tables of $C_{L,inv}(\alpha)$, $C_{L,sep}(\alpha)$ and $f_{stat}(\alpha)$ for the modified Kirchoff flow model:

If $\alpha < \alpha_c$,

$$C_{L,inv} = C_{L\alpha} \cdot (\alpha - \alpha_0)$$

Else $C_{L,inv}$ is taken from equation (3.3.2.2.2).

Equation (3.3.2.2.1) is used to solve for f_{stat} if $C_{L,stat} > \frac{1}{4} \cdot C_{L\alpha}(\alpha - \alpha_0)$.

Then $C_{L,sep} = C_{L,inv} / 4 \Rightarrow$

$$f_{stat} = \left(\sqrt{\frac{4 \cdot C_{L,stat}}{C_{L,inv}}} - 1 \right)^2 \quad (3.3.2.2.4)$$

If $C_{L,stat} < \frac{1}{4} \cdot C_{L\alpha}(\alpha - \alpha_0)$, then

$$f_{stat} = 0 \text{ and } C_{L,sep} = C_{L,stat}.$$

In DYNSTALL, $C_{L,f}$ is then obtained from equation (3.3.2.2.1) as

$$C_{L,f}(\alpha_g) = C_{L,sep}(\alpha_E) + \frac{1}{4} \cdot C_{L,inv}(\alpha_E) \cdot (f_{dyn} + 2\sqrt{f_{dyn}}) \quad (3.3.2.2.5)$$

with f_{dyn} from equations (3.3.2.1.3) and (3.3.2.1.4)

3.3.3 Vortex lift (lvormeth=2)

The vortex lift is calculated with equations equivalent to equations (2.2.3)-(2.2.5) but with equation (2.2.3) replaced with

$$c_v = C_{L,c} - C_{L,f} \quad (3.3.3.1)$$

The feed in vortex lift is further only allowed as long as the angle of attack is increasing. So that the second term in equation (2.2.5) is zero if the angle of attack is decreasing.

Furthermore, negative feed of vortex lift is not allowed. So that if $(c_{v,n} - c_{v,n-1}) < 0$, the second term in equation (2.2.5) is again set to zero.

The feed in vortex lift is furthermore disregarded if the angle of attack is too high. This is controlled by an input variable $\alpha_{shift,ds}$.

In AERFORCE [1] $\alpha_{shift,ds}$ is set to 50° (0.87 rad).

3.3.4 An alternative version of vortex lift (lvormeth=1)

The subroutine vo_sub_c.f also includes a version of vortex lift calculations where the feed in vortex lift stops after a certain time delay after a critical C_N condition has been obtained.

This version of vortex lift calculations also includes criteria for when vortex feed can start again after having been terminated.

Only primary vortex shedding is considered. The method is considered less robust for simulations with stochastic wind for wind turbines. No further explanation of the method is therefore given in this report, and the reader is referred to the code and to [5].

3.4 Unsteady drag

Unsteady drag effects are implemented in DYNSTALL. The unsteady effects on the drag are:

- $C_{D,ind}$. The shed wake induced drag
- $C_{D,sep}$. The change in drag due to the separation point position being different from its static position.
- $C_{D,vor}$. “Vortex drag”. A component of the vortex lift must be added to the drag since vortex lift is assumed to act normal to the chord.

The total drag is taken as:

$$C_D = C_{D,stat} + C_{D,ind} + C_{D,sep} + C_{D,vor} \quad (3.4.1)$$

Induced drag

$C_{D,ind}$ is calculated as the component of lift inclined the shed wake induced angle of attack

$$C_{D,ind}(\alpha_g) = \sin(\alpha_{75} - \alpha_E) \cdot C_{L,f}(\alpha_g) \quad (3.4.2)$$

Separation drag

If the separation point is forward of its static position, then it is assumed that the drag will be less than if the separation point was at its static position and vice versa. This is modeled, more or less as suggested by Montgomerie in [13]:

$$C_{D,sep}(\alpha_g) = A_{cd} \cdot (C_{L,stat}(\alpha_E) - C_{L,f}(\alpha_g)) \quad (3.4.3)$$

A_{cd} is an empiric constant.

Vortex drag

The vortex drag is calculated as

$$C_{D,vor}(\alpha_g) = C_{N,v}(\alpha_g) \cdot \sin(\alpha_g) \quad (3.4.4)$$

With the vortex lift taken as

$$C_{L,vor}(\alpha_g) = C_{N,v}(\alpha_g) \cdot \cos(\alpha_g), \quad (3.4.5)$$

the tangential force component of vortex lift will then be zero.

Versions of how to add dynamic drag effects

An input parameter controls how the unsteady drag effects should be calculated.

If **LCDDYN=0**, then the drag is taken as the static drag

$$C_D(\alpha_g) = C_{D,stat}(\alpha_g)$$

If the unsteady drag is modeled then it is not quite clear if the static drag from the tables of $C_{D,stat}(\alpha)$ should be taken for the geometric angle of attack or for the effective angle of attack, α_E . There are therefore two versions:

LCDDYN=1 :

The static drag is evaluated at the geometric angle of attack:

$$C_D(\alpha_g) = C_{D,stat}(\alpha_g) + C_{D,ind} + C_{D,sep} + C_{D,vor} \quad (3.4.6)$$

LCDDYN=2 :

The static drag is evaluated at the effective angle of attack:

$$C_D(\alpha_g) = C_{D,stat}(\alpha_E) + C_{D,ind} + C_{D,sep} + C_{D,vor} \quad (3.4.7)$$

3.5 Unsteady pitching moment

Unsteady effects on the pitching moment for separated flow effects are not included in DYNSTALL.

The pitching moment that is returned is thus the static pitching moment corrected for attached flow unsteady effects.

$$C_M(\alpha_g) = C_{M,stat}(\alpha_g) + C_{M,I} \quad (3.5.1)$$

with $C_{M,I}$ from equation (3.2.2.9)

3.6 Ways to make the model work for all angles of attack

For simulation of wind turbine loads in design calculations, the wind can in principle come from any direction. The airfoils could therefore be blown at from the rear.

One problem in itself is to generate sensible airfoil data for the whole range of angles of attack. The other problem is to make the dynamic stall model to work for flow (that is 2D flow) at any angle.

First all equations in sections 3.1-3.4 are written so that the dynamic stall works for negative angles of attack in the range $[0^\circ, -90^\circ]$. This comes automatically and only needs some special treatment in the vortex lift calculations. With a decrease in angle of attack in section 3.3.3 is really meant a decrease of absolute values of angle of attack and negative feed of vortex lift refers to the case when the angle of attack is positive.

Moreover, the equations should work for the angle of attack ranges $[-180^\circ, -90^\circ]$ and $[90^\circ, 180^\circ]$.

The angle of attack range $[-90^\circ, 90^\circ]$ is called $\alpha_{case} = 1$ in the code.

The angle of attack range $[-180^\circ, -90^\circ]$ is called $\alpha_{case} = 2$ in the code.
The angle of attack range $[90^\circ, 180^\circ]$ is called $\alpha_{case} = 3$ in the code.

The angle of attack ranges for $\alpha_{case} = 2$ and $\alpha_{case} = 3$ could also be put together in a continuous angle of attack range with the transform

$$\alpha_2 = \alpha + 180^\circ \text{ if } \alpha_{case} = 2 \quad (3.6.1)$$

$$\alpha_2 = \alpha - 180^\circ \text{ if } \alpha_{case} = 3 \quad (3.6.2)$$

In this new angle of attack, both $\alpha = -180$ and $\alpha = +180$, is represented by $\alpha_2 = 0$.

A second lift curve slope and a second zero lift angle of attack, $C_{L\alpha,2}$ and $\alpha_{0,2}$ must therefore be used if α is in the range $[-180^\circ, -90^\circ]$ or $[90^\circ, 180^\circ]$.

For every angle of attack there, thus, also exist a “dynamic stall angle of attack” that goes in the equations for the dynamic stall model. Since the dynamic stall model includes some table looking, the, original angle of attack also is passed to the model.

The dynamic stall model is therefore fed with

α_g , $\alpha_{g,ds}$ and $\alpha_{75,ds}$. $\alpha_{g,ds}$ and $\alpha_{75,ds}$ are the α_2 angles of attack from equations (3.5.1) and (3.5.2) if $\alpha_{case} = 2$ or $\alpha_{case} = 3$. If $\alpha_{case} = 1$, then $\alpha_{g,ds} = \alpha_g$ and $\alpha_{75,ds} = \alpha_{75}$.

$C_{L\alpha}$ and α_0 are also chosen for the respective α_{case} .

3.7 Robustness of the DYNSTALL-methods

Differential equations are solved such that rather long time steps could be used. To get the method work well, the time step should of course be shorter than the time-constants in the equations. The equations are, however, written such that if the time constant is small

in relation to the time step, then the dynamic effects just becomes absent. See e.g. equations (3.3.1.2) and (3.3.1.3) or the equations to calculate the shed wake effects, equations (3.2.2.3) and (3.2.2.5).

In order to simulate the attached flow effects well the time step should be approximately shorter than corresponding to $\Delta s = 0.5$ ($\Delta s = 0.5$ is the step length for the airfoil to move a $\frac{1}{4}$ chord).

3.7.1 Versions that work for all angles of attack

If the dynamic stall model should be used for angles of attack above the range $[-90^\circ, 90^\circ]$, the Øye model (lfmeth=2) does not work.

The modified Kirchhoff model (lfmeth=4) works for the whole range of angles of attack.

4 Input to the FORTRAN subroutine package

The use of the subroutines for dynamic stall is partly described in the description of the AERFORCE blade-element/momentum code program [1]. Much of the same information and some further information is given below.

4.1 Subroutines

The main subroutine in the DYNSTALL-package is the **dyncl_c** subroutine.

This subroutine then in turn calls subroutine **v_esti_c** in file **v_esti_c.f** and the appropriate subroutine for vortex lift in the file **vo_sub_c.f**.

The subroutines work with a number of state-variables. E.g. d_p and $C_{N,pot}$ at the current time step and at the pervious time step (see equation (3.3.1.2). Methods to solve differential equations are such that data only from the previous and current time step are needed)

In order to update values at the current time step to values at the next time step subroutine **cu_2_old_aer_c** in the file **cu_2_old_aer_c.f** is called.

The DYNSTALL-package is intended for use in a blade-element/momentum code and it is called for one blade element at the time. Matrix indices for blade and radial element number are therefore needed (variables IB and IR).

At the first time step, values for state-variables at the previous time step must be set. An example of how this can be made is given in the subroutine **clcd_firstime** in the AERFORCE subroutine package.

4.2 Conventions for variable names.

For the solution of differential equations, variable values at the previous time step is needed. Variable names ending with `_1` refers to variable values at the previous time step.

4.3 About history of variable names

In the code, variable names still bear marks from the first versions of DYNSTALL which worked with C_N and instead of C_L . A variable CNF should perhaps better be called CLF now, and CNSEPIN should perhaps better be called CLSEPIN. The history of the code is hence, not for best readability, still visible.

4.4 Communication with the subroutines

The basic input to the main DYNSTALL subroutine, `dync1_c`, is

- Airfoil data
- Angle of attack, chord and time-step

The basic output is

- Lift, drag and pitching moment coefficients

Some of the variables are communicated as formal parameters to **`dync1_c`**, but the main part are communicated via common areas.

The formal parameters in the subroutine call are explained in the code.

The `dync1_c` subroutine is called from subroutine `clcdcalc_c` in the AERFORCE subroutine package and this gives some information on the use.

4.5 Common areas in Dyncl_c.inc

The file `dyncl_c.inc` includes common-areas with variables that are needed by the dynamic stall subroutines e.g. storage of airfoil aerodynamic coefficients.

4.5.1 Storage of static airfoil data.

The aerodynamic static airfoil data should be stored in data tables $C_L(\alpha)$, $C_D(\alpha)$ and $C_M(\alpha)$. The subroutine package is intended for use with a blade-element/momentum code where track of a specific airfoil table for each blade element is required. Airfoil data are therefore given for one or for more airfoils.

These airfoil data tables are stored in the common area `/profidata996/`

Each airfoil is associated with one table.

Data for at least one airfoil is needed.

Static airfoil data, α , $C_{L,stat}$, $C_{D,stat}$ and $C_{M,stat}$ are stored in variables `alfastin`, `clstin`, `cdstin` and `cmstin`.

For calculation with the dynamic stall model (`lcncl=2`), the static data for C_L is however not used from the $C_{L,stat}$ variable, but from the variables f_{stat} , $C_{L,inv}$ and $C_{L,sep}$ as explained in section 3.3.

If the Øye $f(\alpha)$ relationship is used (`LFMETH=2`), then the input airfoil data tables should include tabulated values of f_{stat} , $C_{L,inv}$ and $C_{L,sep}$ as input. The tabulated values of $C_{L,stat}$ are then ignored.

If the modified Kirchoff flow $f(\alpha)$ relationship is used (`LFMETH=2`), the same also holds. The tables of f_{stat} , $C_{L,inv}$ and $C_{L,sep}$ could, however, then automatically be generated by a call to the subroutine **kirchmake_c**. The subroutine `kirchmake_c` fills the tables `fnstin`, `cninvin` and `cnsepin` (f_{stat} , $C_{L,inv}$ and $C_{L,sep}$).

Airfoil data are stored in matrices `alfastin(ia,ip)`, `clstin(ia,ip)` etc.. The second index refers to a table number. i.e. which airfoil it is. The first index refers to the row number (angle of attack index) in the airfoil data table.

Apart from matrices `alfastin`, `clstin`, `cdstin`, `cmstin`, `fnstin`, `cninvin` and `cnsepin`, data for the zero lift angle of attack lift curve slope is also needed. The zero lift angle of attack and the lift curve slope are stored in the variables `alfa0` and `cn_alfa`. (`cn_alfa` should be in units 1/radians and `alfa0` in radians).

The zero lift angle of attack and the lift curve slope around $\pm 180^\circ$ angle of attack is also needed as input if the angle of attack exceeds $\pm 90^\circ$. These are stored in variables `cn_alfa2` and `alfa02`.

Furthermore the `/profidata996/` area contains `cnlpos` and `cnlneg` which is the critical C_N conditions needed for the vortex lift calculations if the method `LVORMETH=1` is used (see section 3.3.4).

An example of one airfoil data table is shown below²

Alfa	Cl	Cd	Cm
-10.0	-0.8600	0.0150	-0.0375
-4.0	-0.1283	0.0067	-0.0785
-2.0	0.1252	0.0068	-0.0834
2.0	0.6273	0.0073	-0.0925
4.0	0.8748	0.0079	-0.0964
6.0	1.1190	0.0086	-0.0997
8.0	1.3525	0.0102	-0.1014
10.0	1.5349	0.0154	-0.0973
12.0	1.5899	0.0271	-0.0843

² Note that the angle of attack as input to `alfastin(.,.)` should be in radians and not degrees

14.0	1.5957	0.0511	-0.0837
16.0	1.5963	0.0797	-0.0868

This table contains 11 rows. If it would refer to airfoil number 1, then the 11 C_L -values should be stored in `clstin(i,1)` with `i` from 1-11.³

Additional to `alfastin`, `clstin`, `cdstin`, `cmstin`, `fnstin`, `cninvin` and `cnsepin` the variable **`nin(ip)`** (in the same common area as `alfastin` et.c.) is also needed. `nin` tells how many rows that are used in each table. In the example above, `nin(1)=11` should be set.

4.5.1.1 Range of angle of attack in input airfoil tables.

The range of angles of attack in each airfoil data table must cover the angles of attack that will be encountered during the calculations. If an angle of attack is calculated outside the input range, then the program will halt (in subroutine `interp999`) when C_L , C_D and C_M values are sought.

To cover the full 360 degrees range of angles of attack, α should be given in the range [-180,180] degrees.

4.5.1.2 Lift curve slope and zero lift angle of attack

The zero lift angle of attack and the lift curve slope are stored in the variables `alfa0`, `cn_alfa`, `cn_alfa2` and `alfa02`.

The zero lift angle of attack and the lift curve slope are however input to the subroutine `dyncl_c` as formal parameters together with the variable α_{case} (`acase`) as explained in section 3.6.

The variables `alfa0_used` and `clalfa_used` should be set to the appropriate values of `alfa0`, `cn_alfa`, `cn_alfa2` and

³ The table must of course include the full range of angles of attack that will be encountered during the calculations. If an angle of attack is calculated to e.g. 20 degrees and the table with `alfa[-10,16]` is used, then the program will stop.

alfa02. None of the variables alfa0, cn_alfa, cn_alfa2 and alfa02 is, however, actually used in the subroutine dyncl_c or subroutines directly called by dyncl_c.

alfa0_used and clalfa_used should be taken as the zero lift angle of attack and the lift curve slope for the cninvin curve, $C_{L,inv}(\alpha)$ -curve.

4.5.2 Choices between submodels

Variables to store choices for which sub-model to use for the dynamic stall calculations are stored in the common-area /typeparam/ These variables need to be set outside of the dyncl_c subroutine.

Lcncl	This parameter should be set to 2 if the dynamic stall model is used. Lcncl=1 was an old, now removed method.
Lpotmeth	lpotmeth should be set to 3 or 4 to obtain methods as explained in section 3.2.
Lfmeth	lfmeth should be set to 2 or 4 to obtain methods as explained in section 3.3.2.
Lvormeth	lvormeth should be set to 2 or 1 to obtain methods as explained in section 3.3.3 or 3.3.4
Lcddyn	lccdyn should be set to 0, 1 or 2. If lccdyn=0, then C_D will be returned as static C_D . The choices between lccdyn=1 and lccdyn=2 are explained in section 3.4
Ldut	If ldut=0, then the effect of a varying velocity on the separation point position is neglected. The same effect is also obtained by setting f_u to zero.

4.5.3 Coefficients and time constants

The area `/potcoeff/` contains the coefficients for the inviscid circulatory lift response.

`/tfparam/` and `/vorparam/` contain input variables for the separation lag part and the vortex lift part of the dynamic stall model.

`/tfparam/` **tp** Time constant T_p . See section 3.3.1

tf_in Time constant T_f . See section 3.3.2

fpar_i and **fpar_d** are not used any more.

fcrit is not used any more

fufac Constant f_u , see section 3.3.1

acd Constant A_{cd} , see section 3.4

`/vorparam/` **tvo** Time constant T_v . See section 3.3.3

tv1 Time constant used with `lvormeth=1`. See section 3.3.4 and the code

tvs Time constant used with `lvormeth=1`. See section 3.3.4 and the code

4.5.4 Variables used for state variables and other variables needed for internal communication

The areas `/curval/` and `/oldval/` contain variables used for the calculation of the dynamic stall (state variables). Values at the current time step is stored in the variables in `/curval/` and the values at the previous time step is stored in `/oldval/`. None of the variables in `/curval/` or `/oldval/` need to be set outside of the `dyncl_c` subroutine package except for that start-conditions for the `/oldval/-` variables must be set as explained in section 4.1.

4.5.5 Variables in common areas that must be set at each time step outside of the DYNSTALL-package

The two variables **vrel** and **up** in the common area /curval/ must be set at each time step. `vrel(ib,ir)` is V_{rel} for blade element IB and radial position IR (see section 3.2.1). `up(ib,ir)` is the plunging velocity u_p (see section 3.2.2).

4.6 Generation of FNSTIN, CNINVIN and CNSEPIN tables

The tables of $f_{stat}(\alpha)$, $C_{L,inv}(\alpha)$ and $C_{L,sep}(\alpha)$ are needed for the calculation of a dynamic C_L .

If the Øye $f(\alpha)$ relationship is used (LFMETH=2), then the airfoil data for f_{stat} , $C_{L,inv}$ and $C_{L,sep}$ must be included in input files. Values of `alfa0_used` and `clalfa_used` should then be taken as the zero lift angle of attack and the lift curve slope for the `cninvin` curve. **Note that the Øye method, in the current implementation, only works for the $\pm 90^\circ$ range of angles of attack.**

If the modified Kirchhoff flow $f(\alpha)$ relationship (lfmeth=4) is used, tables of f_{stat} , $C_{L,inv}$ and $C_{L,sep}$ can be automatically generated by a call to the subroutine **kirchmake_c**. The subroutine `kirchmake_c` fills the tables `fnstin`, `cninvin` and `cnsepin` (f_{stat} , $C_{L,inv}$ and $C_{L,sep}$).

In the AERFORCE package, `kirchmake_c` is called at the first time step to set up f_{stat} , $C_{L,inv}$ and $C_{L,sep}$ -tables if `lfmeth=4`.

The subroutine `kirchmake_c` also fills the variables of `alfa0`, `cn_alfa`, `cn_alfa2` and `alfa02` from which appropriate values of `alfa0_used` and `clalfa_used` can be selected

5 Sub-methods and values for semi-empiric constants

Reported use of the FFA dynamic stall model is the use in the Stallvib project [3], [11].

The model is also used in a sensitivity analysis [14].

5.1 An optimization study to find optimum values

Optimal parameters for the dynamic stall model was sought by optimization in [15], [16].

In this work experimental data from several sources were used. Values for the semi-empirical constants in the dynamic stall model that would minimize the difference between simulation and experimental results were sought.

In [15] and [16] the Kirchoff flow model was used.

The result was that there is a substantial span in the result of optimum values for the parameters for different airfoils and different cases.

T_v and T_f

One conclusion is that with $T_v \approx 2$ and $T_f \approx 5$, a reasonable good agreement was obtained for a large number of cases.

A_{cd}

Optimum values semi-empirical parameter A_{cd} was found in the range from 0 to 0.43. Most values were below 0.1. A value of $A_{cd} \approx 0.05$ to $A_{cd} \approx 0.1$ seams reasonable to use.

T_p

The value for $T_p=0.8$ was used in most cases in the optimization study [16]. An optimum value was also sought, but the span of optimum values was substantial so that it is hard to recommend a value based on this study. The value $T_p=0.8$ was taken from [10] for plunging motion.

5.2 lccdyn

In calculations for the stallvib project it was found that lccdyn=2 gave better agreement with experimental data than using lccdyn=1

5.3 Effects of varying velocity on the separation point

The model to account for changes in the unsteady pressure gradient due to a varying free stream velocity was introduced during the STALLVIB project. Very limited investigations [11] found a value of the semi-empiric constant $f_u=0.5$ to be reasonable.

f_u should, however, likely be a function of angle of attack or a function of the separation point position. At high angles of attack, a value of $f_u=0.5$ might be too high.

5.4 Recommended values of sub-models and semi-empirical parameters

The dynamic stall model captures several features of unsteady airfoil aerodynamics and dynamic stall. The model is often able to quite well predict the $C_L(t)$ and $C_D(t)$ behavior. The model is, however, not a solution of the flow for the dynamic stall process. Different airfoils might require different values of semi-empirical constants to get a good fit to the real dynamic stall behavior.

Based on experience with the semi-empirical dynamic stall model and based on the experience from the optimization study [16] it

seems a bit unwise to recommend values for the semi-empirical constants for a “general airfoil”. Nevertheless, such values will be asked for so why not give a best guess.

For use in aeroelastic calculations with “common” wind turbine blade airfoils the author’s current default setting is:

$$T_p=0, \quad T_f=5, \quad T_v=2, \quad A_{cd} 0.08, \quad f_u=0.25$$

The choice of sub-models should then be:

$$lcnc1=2, \quad lpotmeth=4, \quad lf meth=4, \quad lvormeth=2, \quad lcddyn=2, \quad ldut=1$$

5.4.1 Effect on aerodynamic damping, fatigue and extreme loads

Sometimes it is good to be a bit on the conservative side in load calculations. How then do the values of the semi-empirical constants affect loads? Unfortunately that is hard to say in general. Some rules of thumb could, however, be given.

5.4.1.1 Damping of flap-wise vibrations in stall

Increase in $T_p \Rightarrow$ increase

Increase in $T_f \Rightarrow$ increase

Increase in $T_v \Rightarrow$ increase

A_{cd} hardly affects the flap-wise damping

f_u does not affect the flap-wise damping

$lpotmeth=4$ instead of $lpotmeth=3$ does not make a big change

5.4.1.2 Damping of edge-wise vibrations in stall

An increase in damping here means more positive or less negative damping.

Increase in $T_p \Rightarrow$ increase

Increase in $T_f \Rightarrow$ increase

T_v hardly affects the edge-wise damping

Increase in A_{cd} => increase

Increase of f_u => decrease

lpotmeth=4 instead of lpotmeth=3 increases the damping.

5.4.1.3 Extreme loads

If the extreme loads increase with increasing maximum values of C_L , then following holds.

Increase in T_p => increase

Increase in T_f => increase

Increase in T_v => increase

A_{cd} hard to say

f_u hard to say

lpotmeth=4 instead of lpotmeth=3: hard to say

References

- [1] Anders Björck. "AERFORCE: Subroutine Package for unsteady Blade-Element/Momentum Calculations", FFA TN 2000-07, The Aeronautical Research Institute of Sweden, June 2000.
- [2] F. Rasmussen, J. Thirstrup Petersen and H. Aagaard Madsen, Dynamic stall and aerodynamic damping, J. Solar Energy Eng. (1999) 121 , 150-155
- [3] Jörgen Thirstrup Petersen, Helge Aagard Madsen, Anders Björck, Peter Envoldsen, Stig Öye, Hans Ganander och Danny Winkelaar. "Prediction of Dynamic Loads and Induced Vibrations in stall", Risoe-R-1045(EN), Risoe National Laboratory, Denmark, 1998
- [4] A. Björck, "Dynamic Stall and Three-dimensional Effects, Final report for the EC DGXII Joule II Project, JOU2-CT93-0345", FFA TN 1995-31, January 1996, The Aeronautical Research Institute of Sweden
- [5] J.G. Leishman and T.S. Beddoes, "A Generalised Model for Airfoil Unsteady Aerodynamic Behaviour and Dynamic Stall Using the Indicial Method", Presented at the 42nd Annual Forum of the American Helicopter Society, Washington D.C. June 1986
- [6] J.G. Leishman and T.S. Beddoes,, T.S. "A Semi-Empirical Model for Dynamic Stall". (A revised version of a paper presented at the 42nd Annual Forum of the American Helicopter Society), Journal of the American Helicopter Society, July 1989
- [7] J.G. Leishman. and G.L. Crouse. "State-Space Model for Unsteady Airfoil Behaviour and Dynamic Stall". Presented

as paper 89-1319 at the AIAA/ASME/ASCE/AHS/ASC 30th Structures, Structural Dynamics and Material Conference, Mobile Alabama, 1989

- [8] Berend Van der Wall and Gordon Leishman, "The influence of Variable Flow Velocity on Unsteady Airfoil behaviour", 18th European Rotorcraft Forum, Avignon, France 1992
- [9] Y.C. Fung, "An introduction to the theory of aeroelasticity", John Wiley and sons, 1955.
- [10] J. T. Tyler and J.G. Leishman, "Analysis of Pitch and Plunge Effects on Unsteady Airfoil Behaviour", Journal of the American Helicopter Society, July 1992
- [11] A. Björck, "The FFA Dynamic Stall Model. The Beddoes-Leishman Dynamic Stall Model Modified for Lead-Lag Oscillations". IEA 10th Symposium on Aerodynamics of Wind Turbines i Edingburgh, 16-17 December 1996. Editor Maribo Pedersen, DTU Danmark
- [12] Stig Øye, "Dynamic stall simulated as time lag of separation", Presented at the IEA Fourth Symposium on the Aerodynamics of Wind Turbines", Rome November 1990, Edited by McAnulty, ETSU-N-118
- [13] Björn Montgomerie, "Dynamic Stall Model Called "Simple", Rep. No. ECN-C--95-060, Netherlands Energy Research Foundation ECN, June 1995.
- [14] A. Björck et al " Computations of Aerodynamic Damping for Blade Vibrations in Stall" Paper Presented at the European Wind Energy Conference, EWEC'97 Dublin, Ireland, October 1997

- [15] A. Björck, M. Mert and H. Aagard Madsen, “ Optimal parameters for the FFA-Beddoes dynamic stall model”
Proceedings of the European Wind Energy Conference, 1-5
March 1999, Nice, France
- [16] Murat Mert , “Optimization of Semi-Empirical Parameters
in the FFA-Beddoes Dynamic Stall Model”,
FFA TN 1999-37, The Aeronautical Research Institute of
Sweden, June 1999

Issuing organization Flygtekniska Försöksanstalten Box 11921 S - 161 11 Bromma Sweden	Document no. FFAP-V-110			
	Date June 2000	Security Unclassified		
	Reg. No. 948/98-23	No. of pages 56		
Sponsoring agency Swedish National Energy Administration	Project no. VU0313	Order/Contract STEM P11556-1		
Title DYNSTALL: Subroutine Package with a Dynamic stall model.				
Author Anders Björk				
Checked by Björn Montgomerie	Approved by Sven-Erik Thor			
<p>Abstract</p> <p>A subroutine package, called DYNSTALL, for the calculation of 2D unsteady airfoil aerodynamics is described.</p> <p>The subroutines are written in FORTRAN.</p> <p>DYNSTALL is a basically an implementation of the Beddoes-Leishman dynamic stall model. This model is a semi-empirical model for dynamic stall. It includes, however, also models for attached flow unsteady aerodynamics. It is complete in the sense that it treats attached flow as well as separated flow. Semi-empirical means that the model relies on empirically determined constants. Semi because the constants are constants in equations with some physical interpretation. It requires the input of 2D airfoil aerodynamic data via tables as function of angle of attack.</p> <p>The method is intended for use in an aeroelastic code with the aerodynamics solved by blade/element method.</p> <p>DYNSTALL was written to work for any 2D angles of attack relative to the airfoil, e.g. flow from the rear of an airfoil.</p>				
Keywords/Nyckelord Aerodynamics, Wind Energy, Unsteady Aerodynamics, Dynamic Stall, Wind Turbine				
Distribution				